

# Nondissociative Chemisorption of Short Chain Alkanethiols on Au(111)

Izabela I. Rzeźnicka, Junseok Lee, Petro Maksymovych, and John T. Yates, Jr.\*

Surface Science Center, Department of Chemistry, University of Pittsburgh, Pittsburgh, Pennsylvania 15260

Received: April 13, 2005; In Final Form: June 13, 2005

The adsorption of methanethiol and *n*-propanethiol on the Au(111) surface has been studied by temperature-programmed desorption (TPD), Auger electron spectroscopy (AES), and low-temperature scanning tunneling microscopy (LT-STM). Methanethiol desorbs molecularly from the chemisorbed monolayer at temperatures below 220 K in three overlapping desorption processes. No evidence for S–H or C–S bond cleavage has been found on the basis of three types of observations: (1) A mixture of chemisorbed CH<sub>3</sub>SD and CD<sub>3</sub>SH does not yield CD<sub>3</sub>SD, (2) no sulfur remains after desorption, and (3) no residual surface species remain when the adsorbed layer is heated to 300 K as measured by STM. On the other hand, when defects are introduced on the surface by ion bombardment, the desorption temperature of CH<sub>3</sub>SH is extended to 300 K and a small amount of dimethyl disulfide is observed to desorb at 410 K, indicating that S–H bond scission occurs on defect sites on Au(111) followed by dimerization of CH<sub>3</sub>S(a) species. Propanethiol also adsorbs nondissociatively on the Au(111) surface and desorbs from the surface below 250 K.

## 1. Introduction

Self-assembled monolayers (SAMs) on solid surfaces have attracted much interest during last two decades due to their wide range of potential applications in such areas as corrosion inhibition, wear protection, biochemical sensors, molecular recognition, and molecular electronics.<sup>1–4</sup> Among many different SAMs which can be prepared, alkanethiols on gold have been frequently used to study the self-assembly process.<sup>5–8</sup> This is because they can easily form highly ordered and stable monolayers. Although a great number of studies contributed to the understanding of the chemisorbed alkanethiols' structure and their physicochemical properties, there is still controversy regarding the nature of the chemical bonding between the S anchor group and the Au substrate, as well as the possibility of disulfide formation<sup>9–11</sup> upon adsorption. In early reports,<sup>12</sup> based on the shape of the potential-energy diagram scaled with the heat of alkanethiol adsorption on Au(111), it has been proposed that S–H bond dissociation may occur for alkanethiols with more than 5 carbon atoms in the hydrocarbon chain. However there has been no experimental proof for hydrogen desorption from such dissociation processes.

Kodama et al.<sup>13</sup> reported the observation of thiolate radical desorption for alkanethiols, containing 6 carbon atoms, from the Au(111) surface. They could not however see significant hydrogen desorption for butanethiol on Au(111).

Many experimental<sup>14–16</sup> and theoretical studies<sup>17–19</sup> have been devoted to methanethiol adsorption on the Au(111) surface. Recent temperature-programmed desorption (TPD) and X-ray photoelectron spectroscopy (XPS) studies by Liu et al.<sup>14</sup> report the dissociative adsorption of CH<sub>3</sub>SH on Au(111) with the formation of methanethiolate species. On the other hand, the results of high-resolution electron energy loss spectroscopy (HREELS) and TPD studies by Nuzzo et al.<sup>15</sup> indicate that methanethiol does not dissociate on this surface. However, some of the vibrational modes observed are unexplained and are a matter of scientific debate.<sup>17</sup> Since these results<sup>14,15</sup> are contra-

dictory, we decided to reinvestigate the system in order to provide a conclusive answer.

In this work, we studied the interaction of methanethiol and *n*-propanethiol in ultrahigh vacuum (UHV) with the atomically clean Au(111) surface by TPD, Auger electron spectroscopy (AES), and low-temperature scanning tunneling microscopy (LT-STM). We provide clear evidence that methanethiol, as well as *n*-propanethiol, adsorb without S–H bond scission on the defect-free Au(111) surface. However, on an Au(111) surface purposely made defective, strong evidence for S–H bond scission is found.

## 2. Experimental Methods

Experiments with TPD and AES were carried out in a UHV chamber equipped with standard surface science analytical tools with a base pressure of  $1 \times 10^{-10}$  Torr. The Au(111) crystal (orientation accuracy =  $\pm 0.4^\circ$ ) was cleaned by argon ion bombardment, followed by annealing to 773 K. The surface cleanliness, as well as the accumulation of sulfur before and after adsorption, was checked by AES and no impurities were found in the depth of Auger sampling at the 1 at. % level.

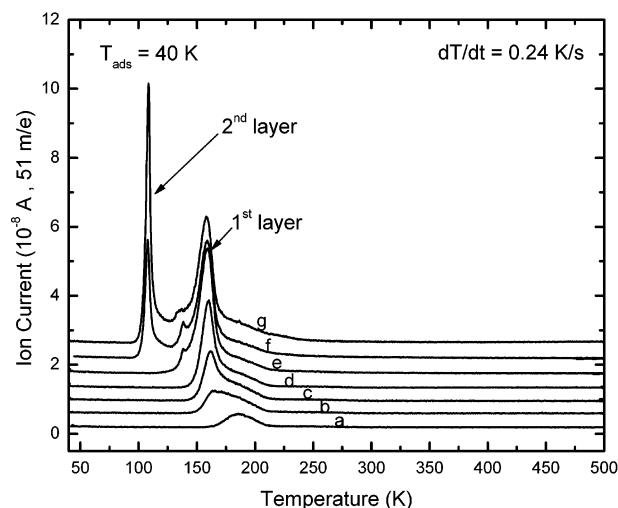
The clean Au(111) crystal was exposed to an equimolar mixture of methanethiol isotopomers (CH<sub>3</sub>SD and CD<sub>3</sub>SH) or *n*-propanethiol at 40 K by use of a calibrated capillary array beam doser.<sup>20</sup> Between each TPD measurement the surface was annealed to 500 K.

A voltage of –70 V was applied to a grid in front of the quadrupole mass spectrometer to eliminate possible damage to the adsorbed layer by stray electrons.

The surface with purposely made defects was prepared by argon ion sputtering without subsequent annealing to high temperature. Prior to adsorption, the ion-bombarded surface was briefly annealed to 200 K in order to remove background contaminants. The fluence of Ar<sup>+</sup> ions (energy = 2 kV) to cause the level of damage used in this investigation was  $1 \times 10^{15}$  Ar<sup>+</sup> cm<sup>–2</sup>.

Scanning tunneling microscopy experiments were conducted at 77 K with an LT-STM (Omicron) operating in UHV

\* Corresponding author: e-mail jyates@pitt.edu.

Temperature Programmed Desorption - CD<sub>3</sub>SH from CD<sub>3</sub>SH+CH<sub>3</sub>SD

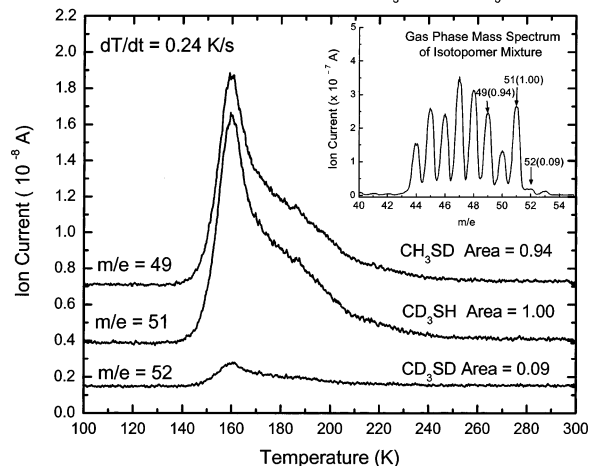
**Figure 1.** TPD spectra of isotopomer mixture of methanethiols (CH<sub>3</sub>SD and CD<sub>3</sub>SH) on the clean Au(111) surface for different exposures: (a)  $6.0 \times 10^{13}$ , (b)  $1.2 \times 10^{14}$ , (c)  $1.8 \times 10^{14}$ , (d)  $2.4 \times 10^{14}$ , (e)  $3.6 \times 10^{14}$ , (f)  $4.8 \times 10^{14}$ , and (g)  $5.4 \times 10^{14}$  molecules/cm<sup>2</sup>.

(background pressure  $< 2.0 \times 10^{-11}$  Torr). The Au(111) crystal was cleaned by Ar<sup>+</sup> sputtering and annealing to 773 K. An effusive beam doser was used to introduce CH<sub>3</sub>SH to the surface while the crystal was in the STM imaging position at 77 K. Minimum data processing was carried out.

### 3. Results and Discussion

**3.1. Adsorption of Methanethiol on Au(111): 3.1.1. Temperature-Programmed Desorption.** Figure 1 shows TPD spectra following CH<sub>3</sub>SD/CD<sub>3</sub>SH mixture adsorption to various coverages on the Au(111) surface at 40 K. Three desorption features are observed in the submonolayer regime with peak maxima at  $\sim 185$ ,  $\sim 160$ , and  $\sim 140$  K. A sharp desorption peak at 110 K is caused by desorption from the condensed multilayer formed on top of the chemisorbed methanethiol layer. The desorption features are consistent with the TPD spectra reported previously for this system.<sup>14,15</sup> The desorption of chemisorbed methanethiol is completed at  $\sim 220$  K and no decomposition products such as hydrogen and methane are observed at higher temperature, in contrast to the study by Liu et al.<sup>14</sup>

The nondissociative adsorption of methanethiol was confirmed in the TPD experiments on an equimolar isotopomer mixture of CD<sub>3</sub>SH and CH<sub>3</sub>SD. If S–H bond dissociation should occur and if recombination then occurred at higher temperature, the fractional production of CD<sub>3</sub>SD ( $m/e = 52$ ) desorbing species should be observed. The results are shown by the multiplexed TPD measurement in Figure 2. The inset displays the gas-phase mass spectrum of the adsorbed isotopomer mixture. A small mass spectral peak due to isotopic mixing, producing CD<sub>3</sub>SD with parent  $m/e = 52$ , is present as a result of the minor exchange reaction occurring in the stainless steel gas handling system used to transfer the gas. If the methanethiol dissociates on Au(111) by S–H bond scission followed by recombination, the ratio of isotopomer yields (52 amu/51 amu = 0.09) in the multiplexed TPD mass spectral scans would differ from that present in the gas mixture. However, no change in the isotopomer ratio is observed when the mixture desorbs from the surface, clearly indicating that methanethiol does not dissociate into thiolate species which then recombine to produce thiol molecules on the Au(111) surface.

Absence of Isotopic Mixing Between CD<sub>3</sub>SH and CH<sub>3</sub>SD - Au(111)

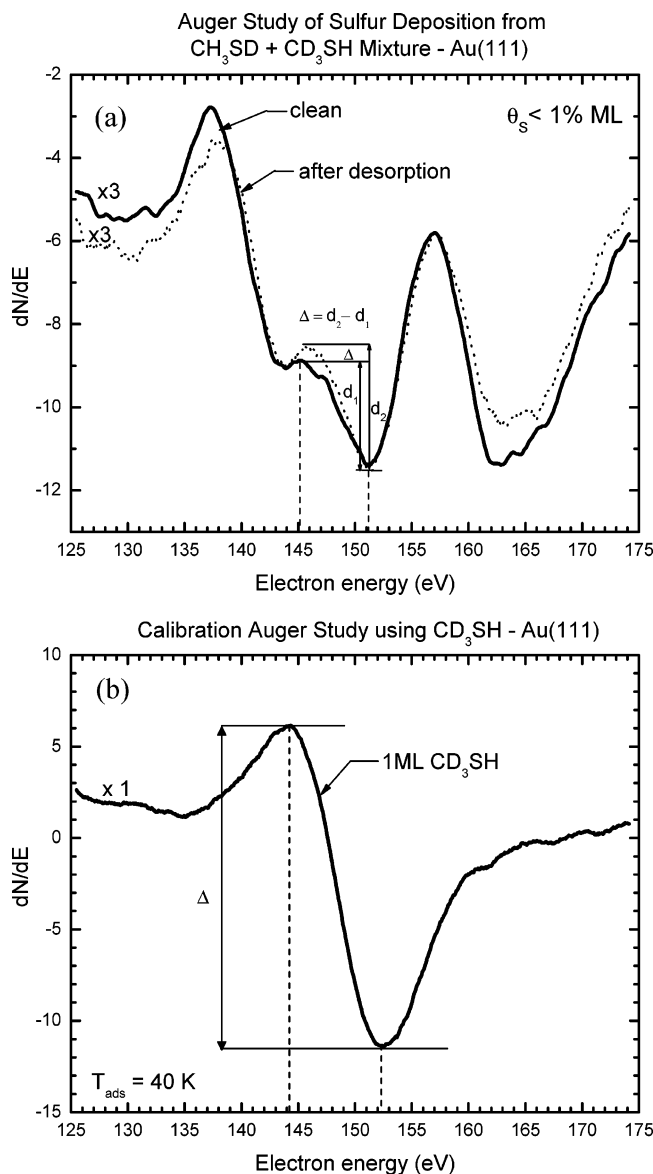
**Figure 2.** TPD spectra of a 50:50 isotopomer mixture of methanethiols (CH<sub>3</sub>SD and CD<sub>3</sub>SH) at submonolayer coverage following adsorption at 40 K, showing the absence of isotopic mixing. (Inset) Mass spectrum of the mixture used for adsorption.

**3.1.2. Auger Electron Spectroscopy Study.** For further confirmation that methanethiol dissociation is absent, AES was performed before and after the TPD process to detect any sulfur accumulation that might appear if the C–S bond is cleaved upon adsorption/desorption. Figure 3a shows the spectra for the sulfur region for the clean Au(111) surface and the surface after desorption of 1 ML (1 monolayer) of methanethiol. The difference, marked by  $\Delta$  in the figure, is proportional to the amount of sulfur that was left on the surface after adsorption and desorption of 1 ML of methanethiol. Figure 3b shows the AES spectrum for 1 ML of the adsorbed methanethiol isotopomer mixture used for calibration of the AES measurement. Comparison of the sulfur intensity in Figure 3 panels a and b indicates that the coverage of sulfur measured after methanethiol adsorption and desorption is less than 1% of a monolayer.

This amount of sulfur is far below the surface coverage required to lift the herringbone reconstruction of Au(111), which recently was reported to be 0.1 ML.<sup>21</sup>

**3.1.3. Low-Temperature Scanning Tunneling Microscopy Study.** To the best of our knowledge this is the first STM study of adsorption of CH<sub>3</sub>SH on Au(111) under UHV conditions. Previous STM work<sup>22</sup> was done on the Au(111) surface in air, exposing the surface to large amounts of CH<sub>3</sub>SH at 300 K. This approach did not allow investigation of the system under controlled surface conditions.

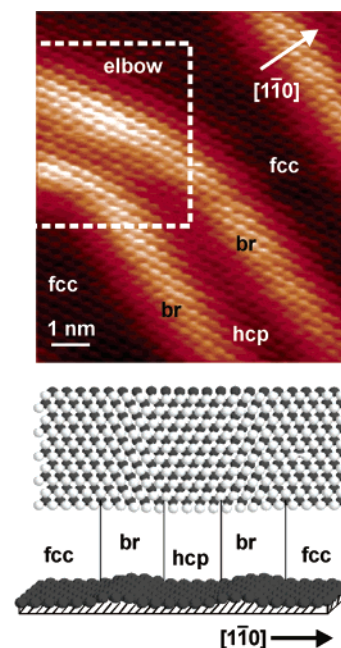
The LT-STM was used in UHV to study the local interaction of CH<sub>3</sub>SH with the atomically clean Au(111) surface, namely, to determine the effect of the  $22 \times \sqrt{3}$  “herringbone” reconstruction of clean Au(111)<sup>23</sup> and the effect of random atomic steps on the adsorption of CH<sub>3</sub>SH. The “herringbone” reconstruction occurs for the atomically clean Au(111) surface, causing a slight buckling of the surface layer of Au atoms along the [110] direction (Figure 4). The buckling causes a periodic change in the vertical stacking of the surface Au atoms from face-centered cubic (fcc) to hexagonal close-packed (hcp) along the buckling direction with regions of faulted stacking, or bridge sites, separating the fcc- and hcp-stacked regions. In addition, due to the 3-fold symmetry and long-range elastic forces on the Au(111) surface,<sup>24</sup> the buckling direction rotates by 120° approximately every 15 nm. The surface region at the point of rotation is referred to as an elbow site, and it contains a number of undercoordinated surface atoms.<sup>23</sup>



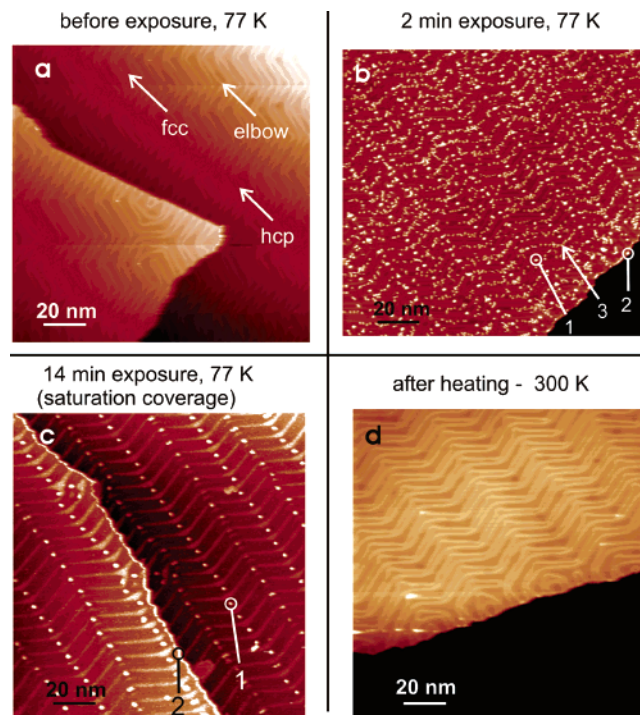
**Figure 3.** AES spectra for sulfur region: (a) before and after TPD (to 500 K) of 1 ML of methanethiol; (b) calibration spectra for 1 ML of methanethiol. The spectra show the absence of S following methanethiol desorption.

Figure 5 shows a series of large-scale STM images taken after exposure of Au(111) at 77 K to  $\text{CH}_3\text{SH}$ . Figure 5a shows the clean Au(111) surface on two terraces separated by an atomic step. Regions of the “herringbone” structures are clearly evident. In Figure 5b, three new types of features due to  $\text{CH}_3\text{SH}$  adsorption are observed on the surface: protrusions on the elbow sites (feature 1), protrusions decorating a random atomic step (feature 2), and numerous identical protrusions on the rest of the surface area (feature 3). At saturation coverage (Figure 5c) the “herringbone” surface structure is maintained and only the features on the elbow and step sites are resolved, while the rest of the surface exhibits fuzzy behavior. This is due to tip-induced motion of  $\text{CH}_3\text{SH}$  molecules on the surface at high coverage. A similar effect was observed with other weakly bound molecules.<sup>25</sup>

The preferential occupancy of particular sites by  $\text{CH}_3\text{SH}$  molecules at 77 K indicates that chemisorption at this temperature occurs via a weakly bound mobile precursor species of  $\text{CH}_3\text{SH}$ . Our observations show that the elbow and step sites are most reactive for  $\text{CH}_3\text{SH}$  adsorption, and the fcc-stacked



**Figure 4.** STM image and schematic of the Au(111)- $(22 \times \sqrt{3})$  “herringbone” reconstruction showing regions of different vertical stacking of surface atoms. Tunneling conditions:  $U_g = 0.33$  V,  $I_t = 0.025$  nA. The schematic diagrams were adopted from ref 32.



**Figure 5.** A series of STM images of the Au(111)- $(22 \times \sqrt{3})$  surface obtained after  $\text{CH}_3\text{SH}$  adsorption at 77 K: (a) clean surface; (b) after exposure for 2 min; (c) after exposure for 14 min; (d) after heating of the  $\text{CH}_3\text{SH}$ -saturated surface to 300 K. In all images  $U_g = 0.32$  V and  $I_t = 0.022$  nA. Species 1, adsorption on the herringbone elbow; species 2, adsorption on the steps; species 3, adsorption on the fcc stacked areas.

regions are more reactive than the hcp-stacked regions and the bridge sites. The observed order of reactivity correlates with a local variation of surface state electron binding energy on the “herringbone” reconstructed Au(111) surface,<sup>26</sup> with greater reactivity corresponding to smaller electron binding energy. A



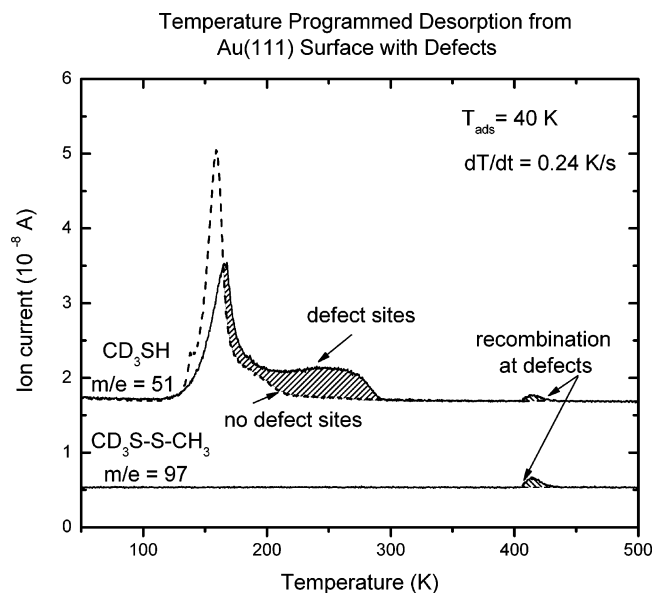


**Figure 6.** TPD spectra of methanethiol on the Au(111) surface with defects produced by 2 kV  $\text{Ar}^+$  bombardment ( $1 \times 10^{15} \text{ Ar}^+ \text{ cm}^{-2}$ ). Exposure:  $3.6 \times 10^{14} \text{ molecules/cm}^2$ .

detailed discussion of these STM results will be presented in a forthcoming publication.<sup>27</sup>

The question of dissociative adsorption of  $\text{CH}_3\text{SH}$  on Au(111) was addressed by observing the effect of heating of the surface with a chemisorbed saturation coverage of  $\text{CH}_3\text{SH}$  up to 300 K. If  $\text{CH}_3\text{SH}$  adsorbed dissociatively by S–H bond scission on Au(111), the resulting  $\text{CH}_3\text{S}$  species would not desorb at 300 K<sup>15</sup> and would therefore be readily observed after subsequent cooling to 77 K.<sup>28</sup> On the other hand, if the  $\text{CH}_3\text{SH}$  adsorption is nondissociative, heating to 300 K should cause complete desorption of the adsorbate (as seen in Figures 1 and 2), producing clean Au(111).

Figure 5 panels c and d show representative STM images obtained before and after heating of the  $\text{CH}_3\text{SH}$ -covered surface to 300 K and subsequent cooling to 77 K. The surface becomes essentially clean, except for an insignificant fraction of bright spots, which are sometimes also observed on a just-prepared surface.

**3.2. Adsorption of Methanethiol on the Au(111) Surface with Defects.** Figure 6 shows the multiplexed TPD spectra after methanethiol adsorption at 40 K on a surface with defects produced by  $\text{Ar}^+$  ion bombardment (followed by heating to 200 K). In comparison to desorption from the surface without defects (dashed line), the  $\text{CH}_3\text{SH}$  desorption process is extended to 300 K, as shown by the crosshatched area under the curve. In addition, the major desorption process near 160 K is diminished as desorption shifts to higher temperature for the defective surface. Moreover, at 415 K, dimethyl disulfide desorption is observed, indicating that a fraction of methanethiol has dissociated on the defect sites and then recombined to form dimethyl disulfide. There is also the desorption of a small amount of methanethiol near 415 K. The origin of the methanethiol at 415 K is a surface reaction involving the thiolate species, since its yield compared to that of the dimethyl disulfide is higher than that expected for the fragmentation of dimethyl disulfide in the ionizer of the mass spectrometer.<sup>29</sup> The formation of dimethyl disulfide was not observed when the defective Au(111) surface was annealed at 500 K, removing surface defects.

The results shown in Figures 2, 3, and 5 clearly indicate that, on a perfect Au(111) surface, methanethiol adsorbs without S–H

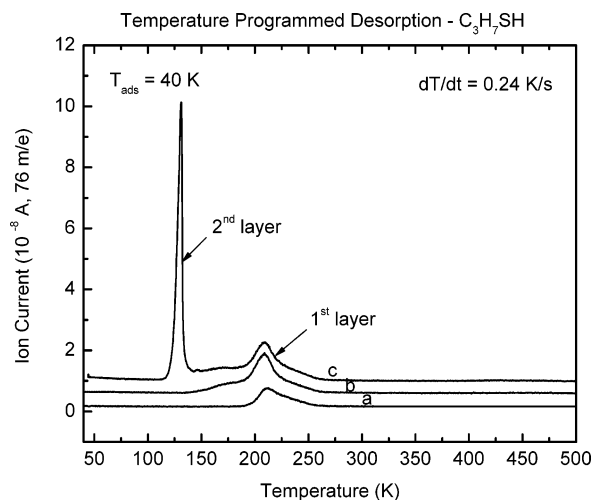


**Figure 7.** TPD spectra of *n*-propanethiol on the clean Au(111) surface for different exposures: (a)  $10.0 \times 10^{13}$ , (b)  $3.0 \times 10^{14}$ , and (c)  $6.0 \times 10^{14} \text{ molecules/cm}^2$ .

and C–S bond scission. In contrast, surface defects on Au(111) made by  $\text{Ar}^+$  bombardment enhance the bonding energy of methanethiol, leading to an increase in desorption temperature and to S–H bond dissociation, producing adsorbed methanethiolate species as shown in Figure 6. Thus, previous reports of  $\text{CH}_3\text{SH}$  dissociation on Au(111) probably reflect the presence of surface defect sites, although our STM measurements indicate that atomic step sites on Au(111) do not cause  $\text{CH}_3\text{SH}$  dissociation.

The question of whether  $\text{CH}_3\text{SH}$  will undergo S–H bond scission at room temperature was addressed by exposing the Au(111) surface to  $\text{CH}_3\text{SH}$  at 300 K with an exposure of  $3.6 \times 10^{14} \text{ molecules cm}^{-2}$ . No dimethyl disulfide desorption was observed. This is similar to results reported for  $\text{CH}_3\text{SH}$  exposure to Ag(110) between 230 and 400 K, where less than 1% of the incident methanethiol molecules dissociated to produce sulfur-containing species.<sup>30</sup>

**3.3. Adsorption of Propanethiol on Au(111).** Similar experiments were performed with *n*-propanethiol,  $\text{C}_3\text{H}_7\text{SH}$ , to determine whether dissociation occurs on perfect Au(111). Figure 7 shows the TPD spectra for  $\text{C}_3\text{H}_7\text{SH}$ . It is noted that the same distribution of desorption processes, compared to  $\text{CH}_3\text{SH}$ , is observed, with both monolayer and multilayer features evident in the desorption spectra. The temperature for the monolayer and multilayer  $\text{C}_3\text{H}_7\text{SH}$  desorption processes is higher than for  $\text{CH}_3\text{SH}$ , due at least partially to the involvement of attractive van der Waals forces between the molecule and the Au(111) surface. These forces would be higher for  $\text{C}_3\text{H}_7\text{SH}$ , due to its higher polarizability, compared to  $\text{CH}_3\text{SH}$ . In addition, experiments similar to that in Figure 6 (not shown), designed to detect the disulfide desorption product  $\text{C}_3\text{H}_7\text{SSC}_3\text{H}_7$ , indicate that this product is not formed on defect-free Au(111).

Auger spectroscopy measurements similar to those shown in Figure 3a for  $\text{CH}_3\text{SH}$  were also carried out before and after the thermal desorption of 1 ML of  $\text{C}_3\text{H}_7\text{SH}$ , and these measurements are shown in Figure 8. Within the accuracy of the AES measurement ( $\pm 0.02 \text{ ML of S}$ ), no residual S is observed on the surface after  $\text{C}_3\text{H}_7\text{SH}$  desorption.

**3.4. Summary of Results.** The experiments reported here indicate that the  $\text{C}_1$  and  $\text{C}_3$  alkanethiols investigated adsorb on Au(111) without dissociation of either the S–H or C–S bonds. The results are similar to the earlier reports for another coinage metal, in which  $\text{CH}_3\text{SH}$  was found to adsorb without dissociation on the Ag(110) surface.<sup>30,31</sup> In addition, the STM results show

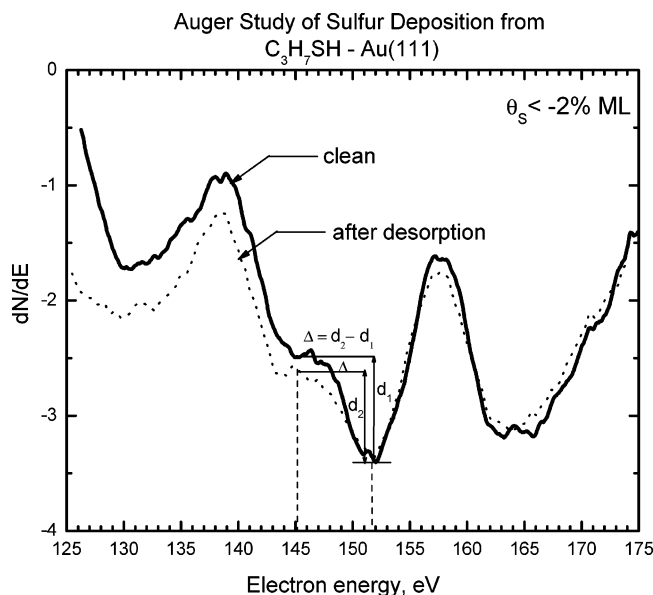


**Figure 8.** AES spectra for the sulfur region before and after TPD (to 500 K) of 1 ML of *n*-propanethiol. The spectra show the absence of S following *n*-propanethiol desorption.

that the mobile  $\text{CH}_3\text{SH}$  molecule exhibits a remarkable chemisorption selectivity for specific Au sites on the reconstructed Au(111) surface at 77 K. In particular, the atomic step sites and the structurally imperfect elbow sites of the “herringbone” reconstruction are most reactive for  $\text{CH}_3\text{SH}$  adsorption, while the fcc-stacked regions of the surface are more reactive than the hcp-stacked regions and the bridge sites.

These observations are important for the theoretical modeling of electrical contact between molecule and metal, where dissociation and formation of alkanethiolate species has been frequently assumed. The accurate description of the nature of the anchor group for SAMs is essential since the sulfur atom hybridization, the surface bond angle, and bond energy will be governed by the presence or absence of the S–H bond at the molecule–substrate interface.

The discovery of the role of surface defects on Au(111) causing S–H bond scission in alkanethiols is also useful in understanding the confusing literature on this issue. Previous reports of thiolate production from short-chain alkanethiols chemisorbed on Au surfaces could reflect the presence of surface defects or the role of other more reactive crystal planes of Au present in polycrystalline substrates.

**Acknowledgment.** We thank the W. M. Keck Foundation for support of this work in the W. M. Keck Center for Molecular

Electronics, located in the Surface Science Center. We also thank NEDO (Japan) for financial support.

## References and Notes

- (1) Ulman, A. *Thin Films: Self-assembly Monolayers of Thiols*; Academic Press: San Diego, 1998.
- (2) Ulman, A. *An Introduction to Ultrathin Organic Films: Langmuir–Blodgett to Self-Assembly*; Academic Press: New York, 1991.
- (3) Schreiber, F. *J. Phys.: Condens. Matter* **2004**, *16*, 881.
- (4) Love, J. Ch.; Wolfe, D. B.; Haasch, R.; Chabynyc, M. L.; Paul, K. E.; Whitesides, G. M.; Nuzzo, R. G. *J. Am. Chem. Soc.* **2003**, *125*, 2597.
- (5) Kato, H. S.; Noh, J.; Hara, M.; Kawai, M. *J. Phys. Chem. B* **2002**, *106*, 9655.
- (6) Engelkes, V. B.; Beebe, J. M.; Frisbie, C. D. *J. Am. Chem. Soc.* **2004**, *126*, 14287.
- (7) Ulman, A. *Chem. Rev.* **1996**, *96*, 1533.
- (8) Dubois, L. H.; Nuzzo, R. G. *Annu. Rev. Phys. Chem.* **1992**, *43*, 437.
- (9) Fetner, P.; Eberhardt, A.; Eisenberger, P. *Science* **1994**, *266*, 1216.
- (10) Noh, J.; Hara, M. *Langmuir* **2000**, *16*, 2045.
- (11) Wan, L.-J.; Hara, Y.; Noda, H.; Osawa, M. *J. Phys. Chem. B* **1998**, *102*, 5943.
- (12) Dubois, L. H.; Zegarski, B. R.; Nuzzo, R. G. *J. Chem. Phys.* **1993**, *98*, 678.
- (13) Kodama, C.; Hayashi, T.; Nozoye, H. *Appl. Surf. Sci.* **2001**, *169*, 264.
- (14) Liu, G.; Rodriguez, J. A.; Dvorak, J.; Hrbek, J.; Jirsak, T. *Surf. Sci.* **2002**, *505*, 295.
- (15) Nuzzo, R. G.; Zegarski, B. R.; Dubois, L. H. *J. Am. Chem. Soc.* **1987**, *109*, 733.
- (16) Duwez, A. S. *J. Electron. Spectrosc. Relat. Phenom.* **2004**, *134*, 97.
- (17) Grönbeck, H.; Curioni, A.; Andreoni, W. *J. Am. Chem. Soc.* **2000**, *122*, 3839.
- (18) Morgner, H. *Langmuir* **1997**, *13*, 3990.
- (19) Franzen, S. *Chem. Phys. Lett.* **2003**, *381*, 315.
- (20) Winkler, A.; Yates, J. T., Jr. *J. Vac. Sci. Technol.* **1988**, *A6*, 2929.
- (21) Biener, M.; Biener, J.; Friend, C. M. *Langmuir* **2005**, *21*, 1668.
- (22) Dishner, M. H.; Hemminger, J. C.; Feher, F. J. *Langmuir* **1997**, *13*, 2318.
- (23) Barth, J. V.; Brune, H.; Ertl, G.; Behm, R. *J. Phys. Rev. B* **1990**, *42*, 9307.
- (24) Bach, C. E.; Giesen, M.; Ibach, H.; Einstein, T. L. *Phys. Rev. Lett.* **1997**, *78*, 4225.
- (25) Böhringer, M.; Schneider, W.-D.; Berndt, R. *Surf. Sci.* **1998**, *408*, 72.
- (26) Bürgi, L.; Brune, H.; Kern, K. *Phys. Rev. Lett.* **2002**, *89*, 176801.
- (27) Maksymovych, P.; Sorescu, D. C.; Dougherty, D.; Yates, J. T., Jr. *J. Phys. Chem. B* (submitted for publication).
- (28) Kondoh, H.; Nozoye, H. *J. Phys. Chem. B* **1999**, *103*, 2585.
- (29) NIST Chemistry Webbook 2003; webbook.nist.gov/chemistry.
- (30) Lee, J. G.; Lee, J.; Yates, J. T., Jr. *J. Am. Chem. Soc.* **2004**, *126*, 440.
- (31) Lee, J. G.; Lee, J.; Yates, J. T., Jr. *J. Phys. Chem. B* **2004**, *108*, 1686.
- (32) Goyhenex, C.; Bulou, H. *Phys. Rev. B* **2001**, *63*, 235404.